CCD Observations and the First Analysis of the Totally Eclipsing, Extreme-Mass-Ratio Binary, GSC 06462-00195

Ronald G. Samec
Pisgah Astronomical Research Institute, 112 Idlewood Acres, Hartwell, GA 30643; ronaldsamec@gmail.com

Daniel Caton
Dark Sky Observatory, Department of Physics and Astronomy, Appalachian State University, 525 Rivers Street, Boone, NC 28608-2106; catondb@appstate.edu

Danny R. Faulkner
Johnson Observatory, 1414 Bur Oak Court, Hebron, KY 41048; dfaulkner@answersingenesis.org

Walter van Hamme
Department of Physics, Florida International University, Miami, FL 33199; Southeastern Association for Research in Astronomy (SARA) Observatory; vanhamme@fiu.edu

Received December 6, 2023; revised January 23, February 8, 2024; accepted May 2, 2024

Abstract GSC 06462-00195 is an eclipsing binary with a mean V magnitude of 11.52, an amplitude of V ~ 0.28 magnitude, a period of 0.6334857 d, and a color index of J–K = 0.211 mag. The ASAS-SN light curve suggests the variable as an extreme-mass-ratio, total eclipsing, W UMa-type binary. Six BVRI eclipse timings were observed with the CTIO reflector, and eight times of low light were taken from ASAS-SN observations. From our present observations, we determined the linear period of 0.63348292 d. Presently, the period appears to be increasing over the 22.2-year period study. A Wilson-Devinney analysis reveals that the system is an A-type (more massive component is the hottest) W UMa-type binary with an extreme mass ratio, q = 0.0937 ± 0.0001. Its fill-out is 66 ± 2%. One hot spot was needed to model a slight light curve asymmetry. The temperature difference of the components is ~416 K. The inclination of ~82.5° results in a long time of totality in the primary eclipse, with a duration of ~109.5 minutes, or 1.82 hours.

1. History and observations

GSC 06462-00195 was originally reported in SIMBAD as an RR Lyrae variable (ATO J063.4331-28.0686). ASAS-SN classifies it as an eclipsing binary with a mean V magnitude of 11.52, an amplitude of V ~ 0.28 mag, a period of 0.6334857 d, and a color index J–K = 0.211 mag. The ASAS-SN light curve (Shappee *et al.* 2016; Jayasinghe *et al.* 2019) shown here as Figure 1 is of low precision; nevertheless it suggests that the system is of low amplitude, yet has a total eclipse. These are the marks of an extreme-mass-ratio binary. Our present study seeks to definitively confirm this.

It appeared in the "80th Name-List of Variable Stars" (Kazarovets *et al.* 2013). The position given there is $\alpha = 04^h\,14^m\,09.0^s$, $\delta = -28°\,11'\,34''$ (2000) and it is correctly given the designation, EW. This system was observed as a part of our student/professional collaborative studies of interacting binaries with data taken from SARA (Southeastern Association for Research in Astronomy, https://www.saraobservatory.org) observations. The BVRI standard Bessel filter light curves were taken by R. Samec and W. Van Hamme with the Cerro Tololo InterAmerican Observatory (CTIO) 0.6-m reflector in the Chilean Andes at an altitude of 2151 m, observed in remote mode, on 2022 December 12 and 13 and 2023 January 28, February 2, 13, and 14, with a thermoelectrically cooled (–50° C) 1KX1K FLI camera. The observations included 685 images taken in B, and 735 in V, 717 in R, and 729 in I. The nightly C–K values stayed constant throughout the observing run with a precision of about 1%. Exposure times were 32–40 s in B, 18–20 s in V, 10–12 s in R, and 10–18 s in I.

A sample of the first ten sets of observations is given in Table 1. The complete table is available through the AAVSO ftp site as given in the table.

The target stars of this investigation, V, C, and K, are identified in Table 2. The finding chart for this field is given in Figure 2. Figures 3 and 4 show plots of nightly light curves on 2022 December 12 and 2023 February 2. The initial study of

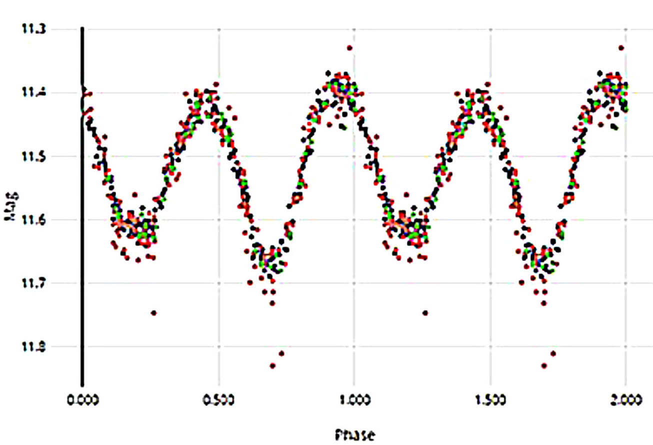

Figure 1. Shallow V light curve of V = ASASSN-V J041343.97-280407.0 = GSC 06462-00195 (Shappee *et al.* 2016; Jayasinghe *et al.* 2019).

Table 1. Sample of first ten GSC 06462-00195 B, V, R, I observations.

ΔB mag (V–C)	HJD 2459900+	ΔV mag (V–C)	HJD 2459900+	ΔR mag (V–C)	HJD 2459900+	ΔI mag (V–C)	HJD 2459900+
–0.965	25.51967	–0.698	25.51320	–0.467	25.52096	–0.329	25.52131
–0.950	25.52203	–0.664	25.51510	–0.490	25.52332	–0.335	25.52367
–0.963	25.52439	–0.688	25.52050	–0.506	25.52572	–0.340	25.52615
–0.965	25.52692	–0.690	25.52280	–0.513	25.52828	–0.340	25.52874
–0.995	25.52952	–0.677	25.52520	–0.514	25.53156	–0.355	25.53203
–0.993	25.53280	–0.703	25.52770	–0.516	25.53416	–0.346	25.53462
–0.981	25.53539	–0.703	25.53030	–0.523	25.53675	–0.345	25.53721
–0.999	25.53799	–0.708	25.53360	–0.524	25.53934	–0.355	25.53980
–0.996	25.54058	–0.713	25.53620	–0.531	25.54193	–0.357	25.54240
–0.996	25.54317	–0.726	25.53880	–0.536	25.54453	–0.356	25.54499

Note: First ten data points of GSC 06462-00195 B, V, R, I observations. The complete table is available through the AAVSO ftp site at ftp://ftp.aavso.org/public/datasets/3917-Samec-521-gsc6462.txt (if necessary, copy and paste link into the address bar of a web browser).

Table 2. The photometric target data.

Star	*Name*	*R.A. (2000)* h m s	*Dec. (2000)* ° ′ ″	*V mag*	*J–K mag*
V (variable)	GSC 06462-00195 ASAS 041344-2804.1 ASASSN-V J041343.97-280407.0 UCAC4 310-004679 2MASS J04134394-2804071[1]	04 13 43.96[2]	–28 04 07.0[2]	11.39–11.71[1]	0.21 ± 0.033[2]
C (comparison)	GSC 06462-00119	04 14 08.98[2]	–28 11 34.9[2]	12.455 (0.03)[2]	0.348 ± 0.047[2]
K (check)	GSC 06462-00944	04 14 01.26[2]	–28 04 7.032[2]	9.752[2]	0.326 ± 0.03[2]

[1] *2MASS (Skrutskie* et al. *2006).* [2] *UCAC3 (Zacharias* et al. *2010).*

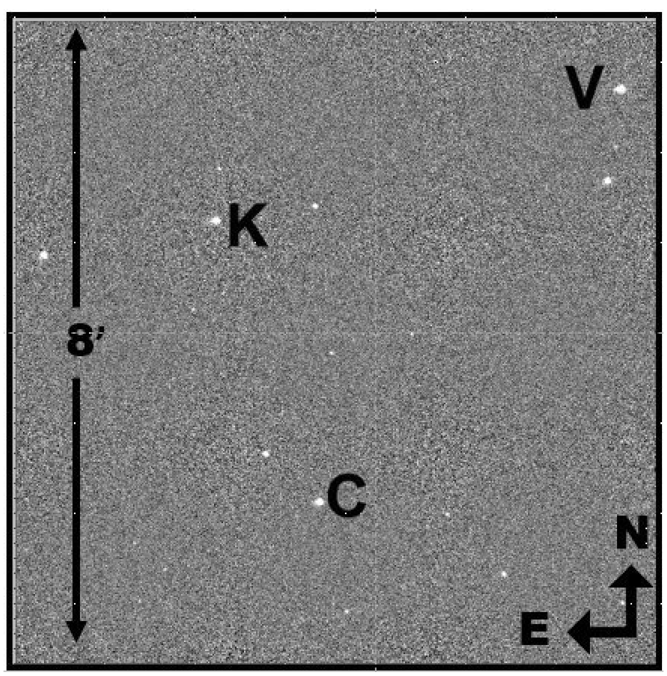

Figure 2. Finding chart of V, the variable star (GSC 06462-00195), C, the comparison star (GSC 06462-00119), and K, the check star (GSC 06462-00944).

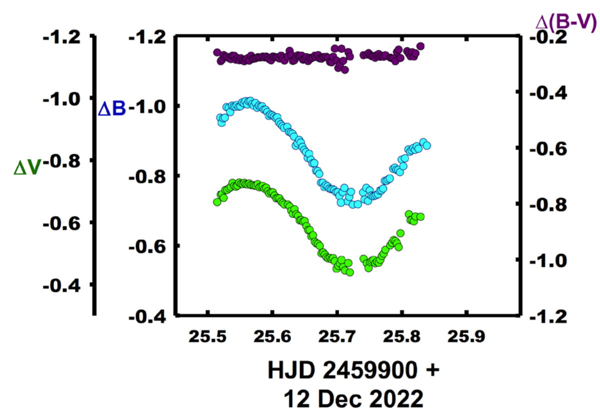

Figure 3. 2022 December 12 observations of GSC 06462-00195.

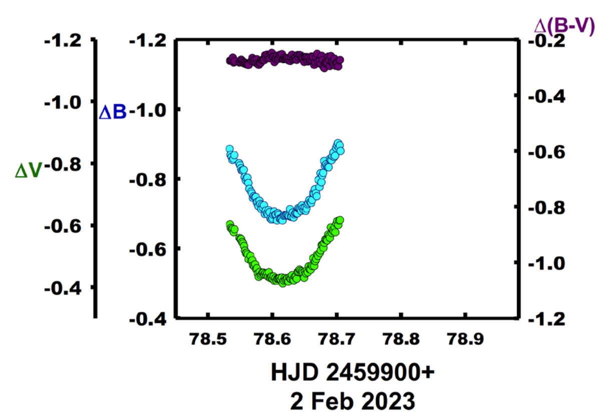

Figure 4. 2023 February 2 observations of GSC 06462-00195.

Table 3. Period study of GSC 06462-00195.

	Epoch	Cycle	Initial Residual	Linear Residuas	Quadratic Residual	Wt	Error	Reference
1	51868.7700	–12802.0	0.0369	0.0013	0.0000	1.0	0.0030	VSX
2	56960.6962	–4764.0	0.0051	–0.0102	–0.0045	0.1	0.0048	ASAS
3	57012.6442	–4682.0	0.0072	–0.0079	–0.0022	0.1	0.0100	ASAS
4	57379.7516	–4102.5	0.0096	–0.0040	0.0013	0.1	0.0040	ASAS
5	57379.7518	–4102.5	0.0098	–0.0038	0.0015	0.1	0.0040	ASAS
6	57566.9467	–3807.0	0.0097	–0.0031	0.0019	0.1	0.0100	ASAS
7	57717.7143	–3569.0	0.0077	–0.0046	0.0003	0.1	0.0040	ASAS
8	57757.6208	–3506.0	0.0046	–0.0075	–0.0027	0.1	0.0060	ASAS
9	57822.5586	–3403.5	0.0101	–0.0017	0.0030	0.1	0.0030	ASAS
10	59925.7289	–83.5	0.0079	0.0044	0.0040	1.0	0.0016	Observations
11	59926.6758	–82.0	0.0046	0.0011	0.0007	1.0	0.0020	Observations
12	59972.6045	–9.5	0.0056	0.0023	0.0017	1.0	0.0014	Observations
13	59977.6803	–1.5	0.0135	0.0102	0.0096	0.5	0.0042	Observations
14	59978.6171	0.0	0.0000	–0.0033	–0.0038	1.0	0.0016	Observations
15	59990.6498	19.0	–0.0035	–0.0067	–0.0073	1.0	0.0041	Observations

this system was given at the 242nd meeting of the American Astronomical Society (Samec *et al.* 2023).

2. Period study

Six times of minimum light were calculated from our present observations, three primary and three secondary eclipses:

$$\text{HJD I} = 2459926.67579 \pm 0.00202\,\text{d},\; 2459978.61705 \pm 0.00162\,\text{d},\; 2459990.64982 \pm 0.00408\,\text{d},$$

$$\text{and HJD II} = 2459925.72888 \pm 0.00161\,\text{d},\; 2459972.60449 \pm 0.00139\,\text{d},\; 2459977.68031 \pm 0.00423\,\text{d}.$$

Eight times of low light were determined from ASAS observations. One time of minimum is given by the International Variable Star Index (VSX; Watson *et al.* 2014). The following linear and quadratic ephemerides were determined from all available times of minimum light:

$$\text{JD Hel Min I} = 2459978.6180 \pm 0.0017\,\text{d} + 0.63348297 \pm 0.00000035 \times \text{E} \qquad (1)$$

$$\text{JD Hel Min I} = 2459978.6209 \pm 0.0010\,\text{d} + 0.633485317 \pm 0.0000010 \times \text{E} + 1.7(0.8) \times 10^{-10} \times \text{E}^2 \qquad (2)$$

The O–C linear and quadratic residual calculations are given in Table 3. Figure 5 gives the plot of epoch vs. the linear residuals. Figure 6 give the plot of epoch vs. the quadratic residuals. The quadratic shows that the period is possibly increasing.

The period study covers some 22.2 years and about ~8000 orbits. The orbit, over this short interval, indicates a period increase at the present time. The shape of the O–C curve following the gap does follow this period change. However, further timings should be undertaken to confirm this trend.

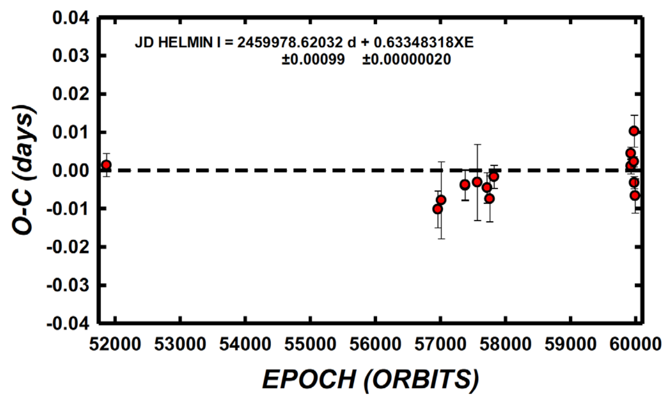

Figure 5. GSC 06462-00195. Plot of epoch vs. the linear residuals.

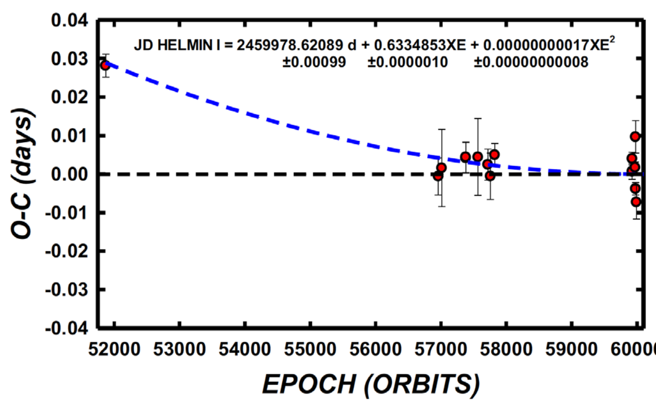

Figure 6. GSC 06462-00195. Plot of epoch vs. the quadratic residuals.

The phased light curves using Equation 1 follow as Figures 7 and 8.

3. Light curve characteristics

The amplitudes of the light curves in all B to I filters are only ~0.31–0.27 mag, which are very small considering the existence of a total eclipse. The O'Connell effect (difference in the maxima), classically believed to be an indicator of spot activity, averages ~0.02 mag in B to I filters, and a minor spot

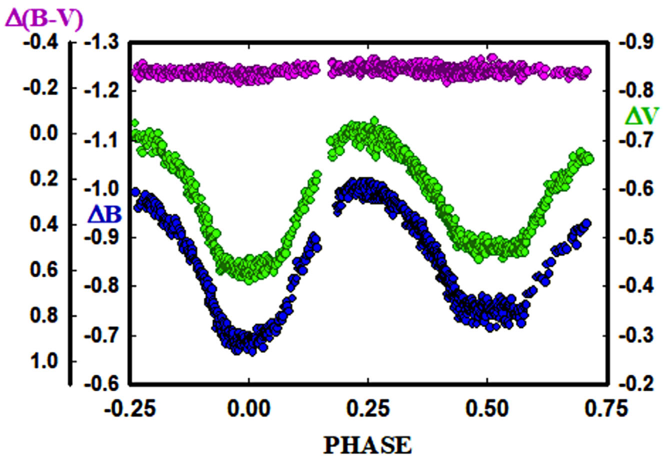

Figure 7. B, V, and B–V color curves of GSC 06462-00195 using magnitudes and Equation 1.

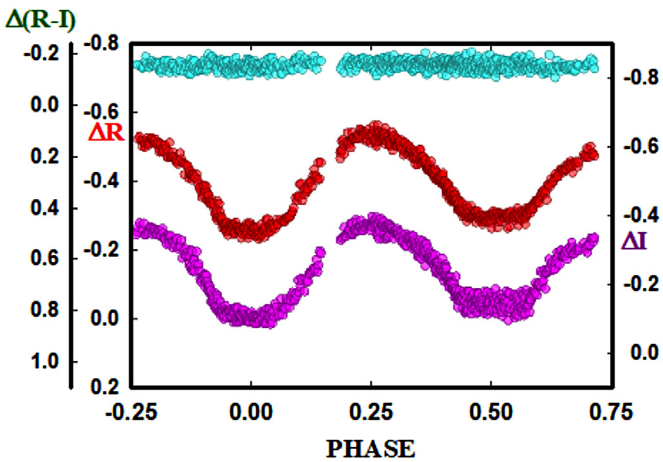

Figure 8. R, I, and R–I color curves of GSC 06462-00195 using magnitudes and Equation 1.

is needed to solve the light curves. The primary and secondary minima show a difference of ~0.07–0.04 mag in B to I, showing that the temperature difference does exist despite the small amplitudes. A total eclipse is very apparent in the secondary minima. The light curve characteristics at quadrature are given in Table 4.

4. Light curve solution

The J–K value of 0.21 (B–V = 0.37) indicates that the binary is of type ~F4V. We used an average primary surface temperature of $T_1 \approx 6750(100)$ K for our synthetic light curve modeling procedure.[1] The B, V, R, and I curves were carefully pre-modeled with Binary Maker 3.0 (Bradstreet and Steelman 2002), producing good fits in all filter bands. The parameters were then averaged and input into a four-color simultaneous light curve calculation using the Wilson-Devinney Program (Wilson and Devinney 1971; Wilson 1990, 1994; van Hamme and Wilson 1998). The solution was computed in Mode 3, the contact mode. Convective parameters, g = 0.32, A = 0.5 were used. Since the eclipses were total, no q-search was performed.

Table 4. Light curve characteristics.

Filter	*Phase Min I*	*Mag σ*		*Phase Max I*	*Mag σ*	
	0.000			0.25		
B	−0.685	±0.008		−0.996	±0.012	
V	−0.437	±0.016		−0.707	±0.015	
R	−0.237	±0.079		−0.534	±0.015	
I	−0.104	±0.010		−0.375	±0.012	
	Min II			*Max II*		
Filter	*Phase*	*σ*		*Phase*	*σ*	
	0.50			0.75		
B	−0.751	±0.013		−0.971	±0.012	
V	−0.480	±0.008		−0.714	±0.015	
R	−0.295	±0.012		−0.513	±0.015	
I	−0.144	±0.020		−0.357	±0.012	
	Min I – Max I	*σ*	*Max II – Max I*	*σ*	*Min I – Min II*	*σ*
B	0.310	±0.020	0.024	±0.024	0.066	±0.022
V	0.271	±0.030	−0.007	±0.007	0.044	±0.024
R	0.297	±0.094	0.022	±0.022	0.058	±0.091
I	0.271	±0.022	0.019	±0.019	0.040	±0.030
	Min II– Max I	*σ*	*Min I – Max II*	*σ*	*Min II– Max II*	*σ*
B	0.245	±0.026	0.286	±0.020	0.220	±0.026
V	0.227	±0.023	0.277	±0.030	0.234	±0.023
R	0.239	±0.027	0.275	±0.094	0.218	±0.027
I	0.231	±0.032	0.253	±0.022	0.212	±0.032

Due to the shallow curves, one important element is the possibility of third light. Thus, third light was explored, but it did not give any meaningful results. We have also investigated the solution with a cool spot, so we reran the program with a cool spot positioned 180° away from the shallow hot spot with a Tfact of 0.92. Solution 2 is given in Table 5. However, the goodness of fit value $[\Sigma(W * Res^2)]$ was poorer. As a result, we give solution 1 as the final solution. The light curve solution table is given in Table 5. Figures 9 and 10 give the plots of the B, V, R, and I light curve solutions overlying the normalized intensities. The Roche Lobe surface geometries at quarter phases follow in Figure 11.

5. Discussion

GSC 06462-00195 is found to be a moderate period, P = 0.6334750(36) d extreme-mass-ratio W UMa-type overcontact eclipsing binary. The relative luminosity in all filters of the primary component has ~90% of the total light. The q ~ 0.0938 mass ratio and its high fill-out (66%) are the main cause of the very shallow amplitude intensities (< 0.2) and the initial false identification as an RR Lyrae variable. According to the light curve solution the more massive component is presently 10.7 times that of the less massive one (q = 0.09). It is thought that the more massive component steadily absorbs the

[1] https://www.pas.rochester.edu/~emamajek/EEM_dwarf_UBVIJHK_colors_Teff.txt

Table 5. B, V, R_c, I_c Wilson-Devinney program solution parameters.

Parameters	*Solution 1*	*Solution 2*
λ_B, λ_V, λ_R, λ_I (nm)	440, 550, 640, 790	440, 550, 640, 790
g_1, g_2	0.32	0.32
A_1, A_2	0.5	0.5
Inclination (°)	82.48 ± 0.11	82.38 ± 0.10
T_1, T_2 (K)	6750, 6334 ± 4	6750, 6390 ± 5
$\Omega_1 = \Omega_2$	1.8990 ± 0.0007	1.8993 ± 0.0007
$q(m_1/m_2)$	0.09377 ± 0.0005	0.09574 ± 0.0004
Fill-outs: F(%)	66 ± 8	74 ± 2
$L_1/(L_1+L_2)_I$	0.8997 ± 0.0005	0.8943 ± 0.0005
$L_1/(L_1+L_2)_R$	0.9033 ± 0.0004	0.8975 ± 0.0004
$L_1/(L_1+L_2)_V$	0.9073 ± 0.0008	0.9011 ± 0.0004
$L_1/(L_1+L_2)_B$	0.9141 ± 0.0004	0.9072 ± 0.0004
JD_o (days)	2459978.62199 ± 0.00012	2459978.61864 ± 0.00012
Period (days)	0.6334750 ± 0.0000036	0.6334793 ± 0.0000037
Dimensions		
r_1/a,	0.5503 ± 0.0007	0.5508 ± 0.0006
r_2/a (pole)	0.2013 ± 0.0016	0.2049 ± 0.0010
r_1/a,	0.6218 ± 0.0012	0.6229 ± 0.0010
r_2/a (side)	0.211 ± 0.002	0.216 ± 0.002
r_1/a,	0.6426 ± 0.0014	0.6444 ± 0.0011
r_2/a (back)	0.267 ± 0.007	0.278 ± 0.008
Spot, Primary	*Hot Spot Region*	*Cool Spot Region*
Colatitude (°)	49.4 ± 1.1	127.0 ± 2.1
Longitude (°)	294.8 ± 0.8	118.3 ± 0.4
Radius (°)	15.2 ± 0.2	22.7 ± 0.2
T-Factor	1.08 ± 0.001	0.917 ± 0.002
$\Sigma(W*Res^2)$	0.63627040	0.64747162

secondary during normal evolution if it follows the expected course. The minimum mass ratio of a W UMa-type binary is thought to be q = 0.071–0.078 (Arbutina 2007). The actual mass ratio is near this range. Kobulnicky *et al.* (2022) state that the q-limit that initiates the collapse is 0.15. However, GSC 06462-00195 may be having an increase in period at the present time. More timings are needed.

With the present mass ratio, a total eclipse would still occur even at a minimum inclination of ~70°. The actual inclination was 82.48 (0.11)° with a long time duration of duration of 1.82 hours.

6. Conclusion

The 22.2-year orbital study (12,800 orbits) of GSC 06462-00195 reveals a possibly increasing period. The increase may be due to the present mass exchange in which mass is flowing to the smaller component. The Wilson-Devinney Program solution gives a mass ratio of ~0.094 and the Roche Lobe fill-out is also extreme, about 66% for this overcontact binary. With this fill-out it is interesting that the component temperature difference is still large, ~416 K. With its small secondary component, the W UMa-type binary is of A-type (the more massive component is hotter).

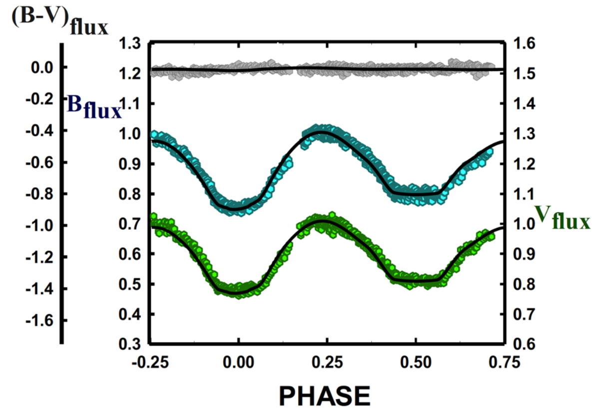

Figure 9. GSC 06462-00195. Light curve solution in B and V overlying the normalized intensities and the color curves, B–V overlying differences.

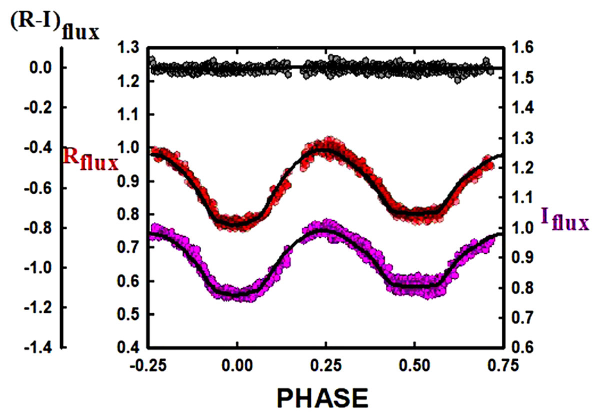

Figure 10. GSC 06462-00195. Light curve solution in R and I overlying the normalized intensities and the color curves, R–I overlying differences.

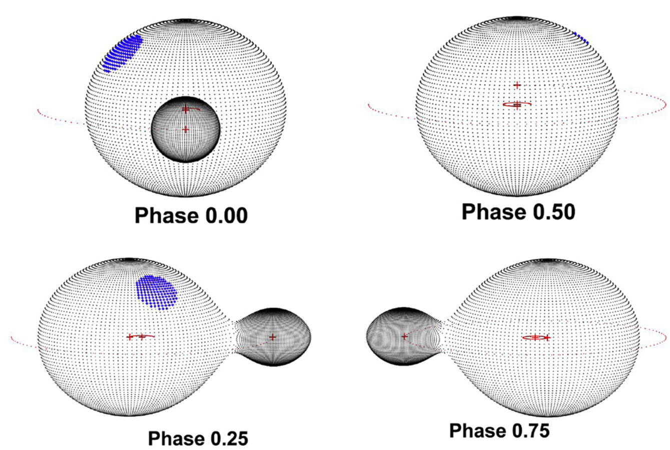

Figure 11. GSC 06462-00195, surface geometry of light curve solution at quarter orbital phases.

7. Future work

Further eclipse timings are need to determine the actual orbital evolution. Radial velocity curves would theoretically allow determination of the binary's absolute elements. Due to the brightness of this system this may not be such a difficult matter. In the future, we will be exploring other binaries with similar light curves.

References

Arbutina, B. 2007, *Mon. Not. Roy. Astron. Soc.*, **377**, 1635.
Bradstreet, D. H., and Steelman, D. P., 2002, *Bull. Amer. Astron. Soc.*, **34**, 1224.
Jayasinghe, T., *et al.* 2019, *Mon. Not. Roy. Astron. Soc.*, **485**, 961.
Kazarovets, E. V., Samus, N. N., Durlevich, O. V., Kireeva, N. N., and Pastukhova, E. N. 2013, *Inf. Bull. Var. Stars*, No. 6052, 1.
Kobulnicky, H. A., Molnar, L. A., Cook, E. M., and Henderson, L. E. 2022, *Astrophys. J., Suppl. Ser.*, **262** 12.
Pojmański, G. 1997, *Acta Astron.*, **47**, 467.
Samec, R., van Hamme, W., Caton, D., and Faulkner D. 2023, *Bull. Amer. Astron. Soc.*, **55**, e-id 2023n2i302p01.
Shappee, B. J., *et al.* 2014, *Astrophys. J.*, **788**, 48.
Skrutskie, M. F., *et al.* 2006, *Astron. J.*, **131**, 1163.
van Hamme, W. V., and Wilson, R. E. 1998, *Bull. Amer. Astron. Soc.*, **30**, 1402.
Watson, C., Henden, A. A., and Price, C. A. 2014, AAVSO International Variable Star Index VSX (Watson+, 2006–2014; https://www.aavso.org/vsx).
Wilson, R. E. 1990, *Astrophys. J.*, **356**, 613.
Wilson, R. E. 1994, *Publ. Astron. Soc. Pacific*, **106**, 921.
Zacharias, N., *et al.* 2010, *Astron. J.*, **139**, 2184.